Time Evolution of the Edge Length Distribution of Networks Generated by Random Transports on a One-Dimensional Lattice

Nobutoshi Ikeda

***Abstract*—** The restriction on the Euclidian edge length is an important consideration in the study of geographical network modeling. We herein investigate a network model developed in a one-dimensional (1-D) lattice, in which the restriction on the Euclidian edge length is a result of dynamical processes on the network, the prosperity of random transports represented by a random walker, and the ageing of edges. Based on numerical calculations, we show that the time evolution of the distribution of the edge length is subject to the 1-D heat conduction equation with a radiation term. According to this equation, the typical equilibrium length of edges is determined by a balance between the diffusion rate and the decrease rate of the edge length density. We can relate these rates to a model parameter that adjusts the aging of edges by comparing the solution of the equation with numerical results. The calculation of the mean shortest path length and the sum of the edge length along the shortest paths shows that the model assumption provides a large traffic capacity on the network and an automatic mechanism causes a natural extinction of the unapproachable area for the walker with the consequent removal of circuitous routes with long edges. The calculation of the clustering coefficient also reveals that the local clustering strength on each vertex is stabilized for a certain value, regardless of the vertex degree. These global and local properties of resulting networks emerge spontaneously from random events in the network, the movement of the random walker, and the aging of edges.

***Keywords*—** Network modeling, Euclidian length of edges, heat conduction equation, random walk, clustering coefficient.

I. Introduction

DIVERSE systems in the real world, such as the Internet, species that interact socially, technological systems, and biological systems, can be modeled by networks in which individuals constituting the system are regarded as vertices and interactions between individuals are regarded as edges [1], [2], [3]. For the last two decades, common network structures in different systems have been discovered. For example, the power law observed in vertex degree distributions of various systems is known as the scale-free property (the vertex degree indicates the number of edges connected to the vertex), and networks with both a large clustering coefficient and a small mean shortest path length between vertices are known as small-world phenomena. Studies on processes in networks have clarified that network structures play an important role in the functions of processes such as spreading processes, synchronization, and tolerance to errors and attacks [4]. Therefore, studies on network structure can help to provide fundamental insights in various research fields.

Network modeling is an effective tool for clarifying the principles behind common properties of various networks. For example, the scale-free property can be described using a simple rule, that is, vertices of large degree tend to gain more new links than vertices of small degree [5]. While random networks intrinsically have small mean shortest path lengths with respect to network size, adding small fractions of random links can reduce the mean shortest path length, even for lattice type geographical networks [6]. However, the simple addition of random links does not allow for sufficient consideration of the geographical properties of networks, because this produces only a uniform distribution of edge length. The Euclidian edge length distribution is an important characteristic in real geographical networks, such as airport networks and highway networks [7], [8], [9], because the Euclidian edge length distribution reflects the spatial constraints on the network topology that are specific to the system. An interesting problem is encountered when rewiring between vertices in a lattice. Specifically, the question arises as to what distribution of length of edges added to a lattice can lead to small-world property in geographical networks [10], [11]. However, previous studies introduced a specific form of the edge length distribution in the first place. The emergence process of the Euclidian length distribution of edges has not yet been investigated.

In the present paper, we investigate the time evolution of the edge length distribution in a network model in which random walkers' movements stimulate shortcuts between vertices on lattice points. This model was proposed in order to consider the increase and decrease in the strength of links in networks due to the prosperity of random transports, and this model was primarily investigated with respect to topology, such as the degree distribution [12]. Modified versions of this model, in which the dimension of the initial lattice was extended [13] and a field affecting the random transports were considered in a one-dimensional (1-D) lattice [14], have been also investigated. However, the geographical aspects of networks, such as the Euclidian length of edges, have been overlooked. Although the present paper considers only a special case of a 1-D lattice, the model provides an example of the emergence process of the edge length distribution resulting from a dynamical process in a networked system.

The remainder of the present paper is organized as follows. Section II explains the model. In Section III, the time evolution

N. Ikeda is with the Department of Living and Culture, Junior College Division, Tohoku Seikatsu Bunka College, Izumi-ku, Sendai 981-8585, Japan (e-mail: nobikeda@mishima.ac.jp).

Manuscript received December 31, 2010.

of the graph and the degree distribution are reviewed. Although most of the results presented in Section III have been reported in our preceding study [13], these results are needed in order to understand the following sections. The primary novel results of the present paper are introduced in Sections IV and V. In Section IV, phenomenological equations describing the time evolution of edge length distribution are derived from an investigation of the time series of the maximum and mean lengths of edges. In Section V, after an explanation of the mean shortest path length between vertices, the sum of the edge length along the shortest path length, and the clustering coefficient, the phenomenological equation is interpreted based on the numerical results obtained for these quantities. Section VI presents a summary of the results.

II. Model

The rules that generate the graph investigated in the present paper are as follows [12]. Initially, a random walker starts from one vertex in a 1-D lattice. The walker is able to move randomly from one vertex to another directly connected vertex in one time step. The process that regulates the addition and removal of edges at each time step is divided into the following three parts:

- Creation of edges. At each time step, a shortcut is created between the vertex at which the walker is currently located and the vertex at which the walker was located two times steps earlier (shortcut creation) as long as an edge does not already exist between these vertices. The random walker is assumed to be able to pass through not only edges in the initial lattice but also newly created edges. In the following, we refer to these vertices, which have gained additional edges due to the passage of the walker as vertices with created edges. In the present paper, we focus primarily on the subgraph that consists of vertices with created edges.
- Strengthen of edges. Each edge is associated with an integer 'strength'. Initially, strength 1 is assigned to newly added edges. At each time step, the strength of two edges is increased by 1. One of these edges is the edge that the walker has passed. The other edge is the edge, if such an edge already exists, that connects the vertex at which the walker is currently located and the vertex at which the walker was located two times steps earlier.
- Aging of edges. At each time step, each strength of the edge is decreased by 1 with probability $p_{\rm d}$. Edges that attain strength 0 are removed, with the exception of edges constituting the 1-D lattice, which exist from the initial time. These exceptional edges are assumed to maintain their strength with the minimum value of 1. This assumption guarantees the permanent maintenance of the 1-D structure in the resulting networks.

The principal characteristic of this model is that the increase and decrease in the vertex degree is determined by the frequency of the walker visiting the vertex. While vertices of large degree are likely to attract the walker via their edges, vertices lose their added edges continuously without the walker's visiting.

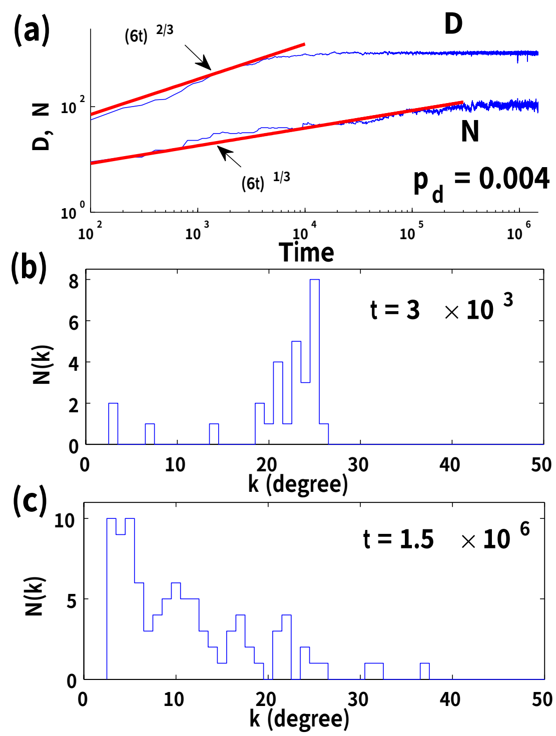

Fig. 1. (a) Time dependence of the sum of degrees on vertices with created edges D and the number of vertices with created edges N. In the first stage of the network evolution, N is described by $(6t)^{1/3}$, which is indicated by the lower straight line. The relation $D \simeq N^2$ indicated by the upper straight line implies the creation of a nearly complete subgraph. Just after the relation $D \simeq N^2$ no longer holds, the next stage of the network evolution begins. (b) Typical degree distribution of the subgraph $N(k)$ (number of vertices in the subgraph of degree k) in the first stage of the network evolution ($t = 3 \times 10^3$, $p_{\rm d} = 0.004$). (c) Typical degree distribution of the subgraph in the third stage of the network evolution ($t = 1.5 \times 10^6$, $p_{\rm d} = 0.004$). The plot of $N(k = 2) = \infty$ is omitted in these figures.

III. Time Evolution of the Graph

The time evolution of the graph is obviously dependent on the rate of diffusion of the walker because a vertex over which the walker has passed can gain a new edge at each step. Note that, as explained in the previous section, the walker is able to pass not only through edges constituting the initial lattice but also through shortcuts that were created by movements of the walker. Therefore, the movement of a random walker is always restricted by past movements of the walker. Consequently, the subgraph consisting of all of the vertices with created edges, which is embedded in the 1-D lattice, evolves through three distinct stages, as follows.

References [13], [15] reported that, in the first stage of the time evolution, a nearly complete subgraph spreads in the 1-D lattice such that $N = (6t)^{1/3}$, where N is the number of vertices with created edges and t is an integer denoting the number of time steps. This behavior is illustrated in Fig. 1(a) as a straight line in the log-log plot. The nearly complete subgraph consists of N continuously aligned vertices, most of which are connected to each other, that are centered at the start point of the walker. The vertex degree distribution in this stage is a function with a peak at N (Fig. 1(b)).

The next stage of network evolution begins when the condition $N = 2\sqrt{1/p_d}$ is satisfied. This stage is characterized by the collapse of the nearly complete subgraph created during the first stage owing to the impossibility of maintaining a complete subgraph under the condition whereby $N > 2\sqrt{1/p_d}$. This is because, under this condition, the rate of decrease of the sum of edge strengths $p_d N(N-1)/2$ is larger than 2, the rate of increase of the edge strength per time. The balance of the decrease and increase of the sum of strength on the edges leads to stagnation of the increase in the number of created edges. Consequently, the number of created edges fluctuates around an equilibrium value, whereas the number of vertices with created edges continues to increase gradually.

In the third stage of the network evolution, the number of vertices with created edges also reaches an equilibrium value. The equilibrium state of the number of created edges and the number of vertices with created edges also implies an equilibrium distribution of the vertex degree with a constant mean vertex degree. Fig. 1(c) illustrates one example of such a degree distribution. Note that the broad shape of the distribution is different from binary distributions obtained by random linking of N vertices.

As might be expected, the time evolution of the edge length distribution is closely related to the change in structure of the subgraph described herein. Therefore, these three stages of network evolution must be kept in mind in order to interpret the calculations in the following sections.

IV. Distribution of Euclidian Length of Edges

The Euclidian distance between two vertices is assumed to be measured in the initial 1-D lattice, in which all of the vertices are located at a constant interval of 1 along a straight line. Then, the Euclidian edge length distribution $E(l)$ (number of edges of Euclidian length l) always takes an infinite value at $l = 1$ for the free boundary condition of the 1-D lattice. Therefore, only edges longer than 2 are considered in the following discussion.

A. Time Series of the Maximum Edge Length and the Edge Length Distribution

In the first stage of network evolution, an analytical form of the Euclidian edge length distribution can be easily obtained as $E(l) \sim (N-l)$ for $(1 \leq l \leq N-1)$ and $E(l) = 0$ for $(N \leq l)$ due to the simple structure of the nearly complete subgraph. The maximum length of edges, which is a parameter that characterizes the edge length distribution in this stage, is subject to time dependence proportional to $N \sim t^{1/3}$, as explained in the previous section. However, the distribution begins to change to a broad-type distribution after entering the second stage of network evolution. The numerically obtained time series of the maximum length of edges yields some valuable information about the edge length distribution, as follows.

Figure 2(a) shows an example of a time series of the mean edge length and the maximum edge length, which change irregularly with respect to time. Therefore, the time series of the shape of the distribution also changes irregularly with respect to time, corresponding to the irregular changes in

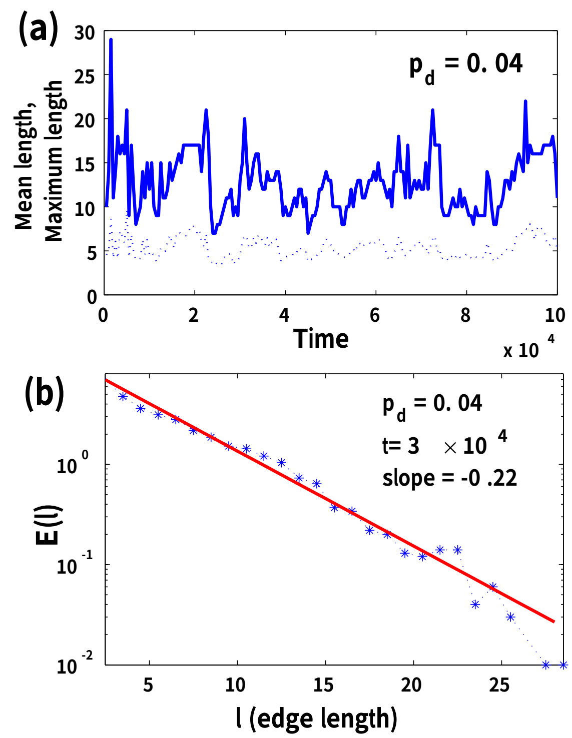

Fig. 2. (a) Example of a time series obtained for the mean edge length (dotted line) and the maximum length (solid line) when $p_d = 0.04$. (b) Edge length distributions $E(l)$ at $t = 3 \times 10^4$ (in the third stage of network evolution) averaged over 100 calculations when $p_d = 0.04$.

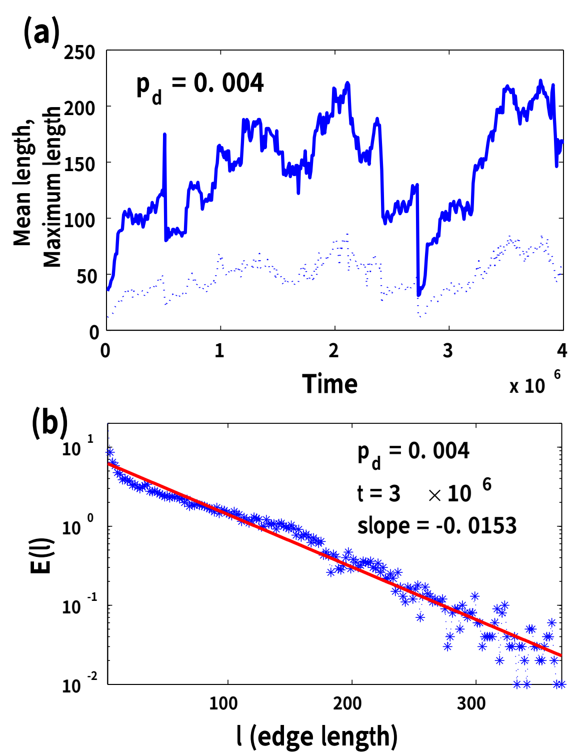

Fig. 3. (a) Example of a time series obtained for the mean edge length (dotted line) and the maximum length (solid line) when $p_d = 0.004$. (b) Edge length distributions $E(l)$ at $t = 3 \times 10^6$ (in the third stage of network evolution) averaged over 50 calculations when $p_d = 0.004$.

the maximum length. However, the distribution obtained by repeated calculations suggests that the edge length distribution can be approximated by an exponential decay (Fig. 2(b)). As $p_{\rm d}$ decreases, a detailed understanding of the changes in the maximum length begins to appear, as shown in Fig. 3(a). The figure shows a sudden decrease in the maximum length of edges after a slow increase, which occurs repeatedly. This result implies that edges that exceed a certain length can exist only in an unstable state, while the distribution obtained by repeated calculation has a finite probability for the existence of such long edges (Fig. 3(b)).

The sudden decrease in the maximum length implies that the longest edge that connects vertices that are far from each other has been removed. One example of such a removal of long edges is illustrated in Fig. 4. On the other hand, the slow increase in the maximum edge length and mean edge length implies that edges tend to be rewired to longer edges. The exponent that characterizes the shape of the distribution is expected to be determined by competition of these two effects, namely, the removal and expansion of edges. The parameter that adjusts these conflicting effects is $p_{\rm d}$. Figure 5 shows the dependence of the characteristic length of edges on $1/p_{\rm d}$, according to which the edge length distribution is approximated as

$$E(l) \sim \exp\left(-p_{\rm d} l/a\right), \qquad (1)$$

where $a/p_{\rm d}$ is regarded as a characteristic length of edges, and parameter a is estimated to be approximately 0.29 in Fig. 5.

B. Phenomenological Equation Describing Edge Length Distribution

The concept that the typical edge length is determined by the balance between the rate of removal of edges and the expansion rate of the edge length provides a means by which to deduce an equation describing the time evolution of the edge length distribution. According to this concept, the increment of the number of edges of length l is the sum of the number of edges that have been rewired from edges of length $l+1$ or $l-1$ to that of l, and the net number of edges of length l that have been removed. Therefore, given that changes in the distribution with respect to t and l are slow enough to enable the continuous approximation to be applied, the balance equation for $E(l,t)$ is

$$\frac{\partial E(l,t)}{\partial t} = -\frac{\partial j(l,t)}{\partial l} - hE(l,t), \qquad (2)$$

where $j(l,t)$ is the flux of the edge length density with respect to the l axis, and h is the net decrease in the ratio of edges of length l per unit time.

For the detection of the behavior of the flux $j(l,t)$ it is helpful to calculate the temporal rate of increase in mean length of edges when $p_{\rm d}$ is so small that a sudden decrease in the maximum length is hardly noticeable. As shown in Fig. 6, the mean and maximum edge lengths are approximately proportional to $\sim t^{1/2}$. In other words, the changes in l behave as a normal diffusion. This is not a trivial result, because this is not the diffusion of the random walker, but rather the diffusion

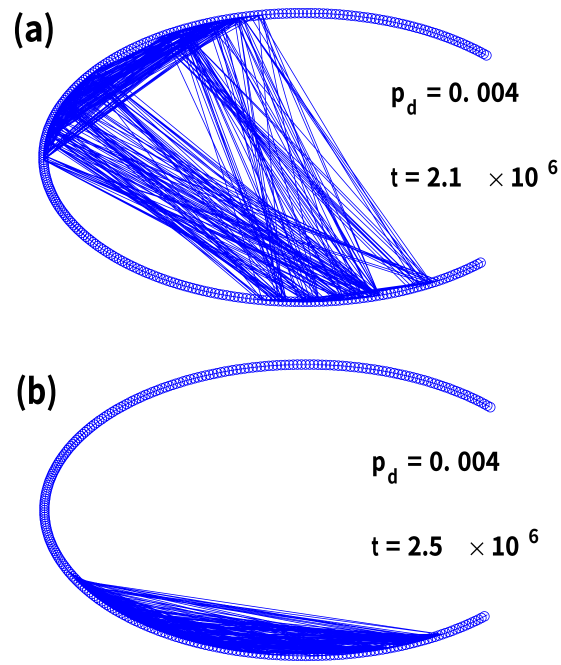

Fig. 4. Two subgraphs realized in the time series indicated in Fig. 3. The oval enclosing the vertices appears strictly for the purpose of visualization, and all vertices are actually assumed to be aligned along a straight line with a constant interval. (a) Subgraph near a local maximum point of the maximum edge length ($t = 2.1 \times 10^6$). (b) Subgraph just after the sudden decrease of the maximum edge length ($t = 2.5 \times 10^6$) showing that some long edges have been removed.

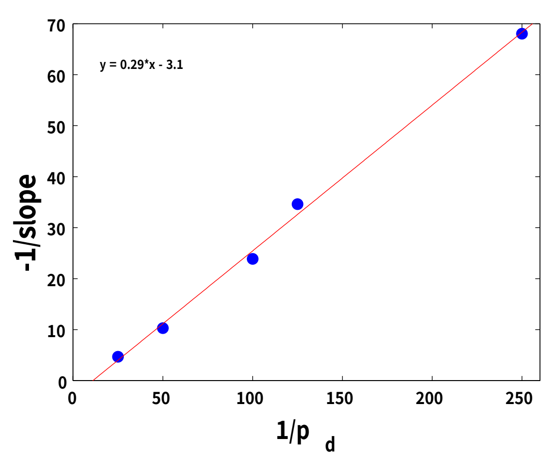

Fig. 5. Numerically obtained characteristic length defined by a reciprocal number of slopes in semi-log plots of the edge length distribution (in the third stage of network evolution) versus $1/p_{\rm d}$.

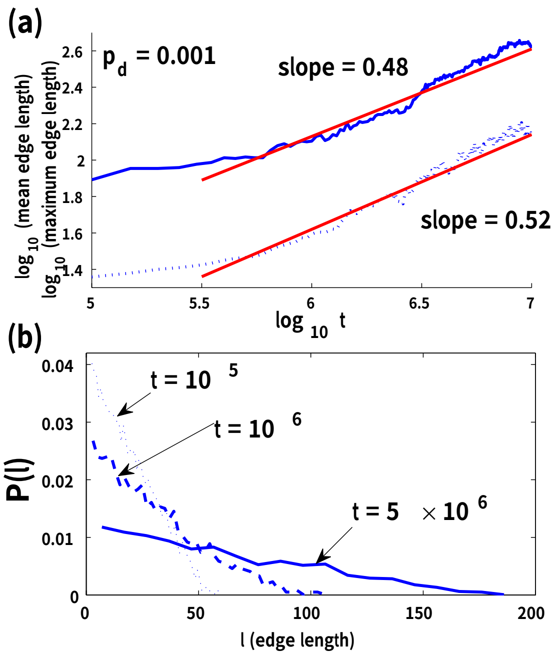

Fig. 6. (a) Log-log plots of the time dependence of the mean edge length and the maximum edge length when $p_{\rm d} = 0.001$. The slopes become approximately 0.5. (b) Normalized edge length distribution $P(l)$ obtained when $p_{\rm d} = 0.001$. At $t = 10^5$ in the first stage of network evolution, as expected, the distribution is triangular. From $t = 1 \times 10^6$ to $t = 5 \times 10^6$, the width of the distribution spreads at a rate of $\langle l \rangle \sim t^{1/2}$, as shown in (a).

of the length of the created edges. The changes in l are a consequence of the cumulative effect of the past movement of the random walker. As a result, the flux is expected to be of the following form:

$$j(l,t) = -D\frac{\partial E(l,t)}{\partial l}, \tag{3}$$

where D is a parameter describing the rate of diffusion of the edge length in l space. With (2) and (3), we obtain a phenomenological equation describing the time evolution of the edge length distribution, as follows:

$$\frac{\partial E(l,t)}{\partial t} = D\frac{\partial^2 E(l,t)}{\partial l^2} - hE(l,t). \tag{4}$$

This equation is similar to the heat conduction equation for a one-dimensional thin rod with outer heat conduction through the lateral surface of the rod [16]. The boundary condition is

$$E(l = \infty, t) = 0, \tag{5}$$

$$D\frac{\partial E(l \simeq 2, t)}{\partial l} = -h\int E(l,t)dl = -hE, \tag{6}$$

where the number of created edges E is approximately constant because the graph is entering the second or third stage of evolution. The boundary condition (6) expresses the situation in which the decrease in the number of edges is compensated by the creation of new edges with the shortest length. However, the left-hand side in (6) must be estimated using a region near $l = 2$, but not just on $l = 2$, because $l = 2$ is so close to the singular point $l = 1$, at which $E(l = 1) = \infty$, that the theory does not work at this point.

Comparing the stationary solution for (4), $\sim e^{-\sqrt{h/Dl}}$, with the numerical results (1), parameters D and h can be related to $p_{\rm d}$ in the following form:

$$D/h \sim 1/p_{\rm d}^2. \tag{7}$$

Here, the decrease ratio h can be related to the lifetime of the edges in l space, τ, via the following relation: $(1-h)^t = e^{(t\log(1-h))} \simeq e^{-ht}$ as

$$h \simeq 1/\tau. \tag{8}$$

Considering that D is expected to decrease as $p_{\rm d}$ decreases, Eqs. (7) and (8) show that the lifetime τ is a very rapidly increasing function as $p_{\rm d} \to 0$.

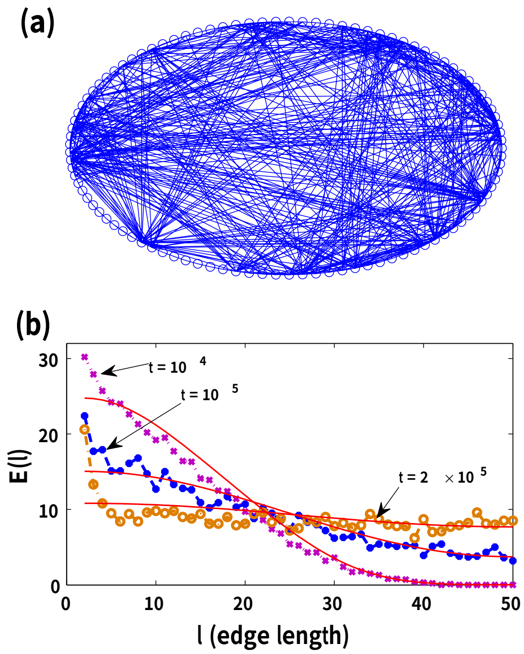

Fig. 7. (a) Typical graph obtained when a periodic boundary condition with a period of $L = 101$ is imposed ($p_{\rm d} = 0.004, t = 2 \times 10^6$). (b) Edge length distribution obtained by 100 calculations ($t = 10^5$, $t = 10^6$, and $t = 2 \times 10^6$) when the periodic boundary condition is imposed. The analytical solution for (9) with the initial condition of triangular form $E/2L + 4LE\sum_n (1 - \cos(\pi n M/L))\exp(-\pi^2 n^2 T/L^2)\cos(\pi n l/L)/(Mn\pi)^2$ is superimposed, where $M = 30$, $L = 50$, $T = 20$, 200, or 500 (solid lines). Decreases in the number of edges that are shorter than a certain value are compensated by increases in the number of edges that are longer than the value.

Here, the question arises as to whether Eq. (4) is applicable to cases with different boundary conditions. However, Eq. (4) is not applicable the case of a periodic boundary condition. A periodic boundary condition is achieved by taking L vertices located on a ring as an initial lattice. In this case, the length of the created edges is limited in the range $2 \leq l \leq [L/2]$. Figure 7(a) illustrates a typical graph created under the condition that all the number of vertices L in the lattice is approximately equal to the equilibrium number of vertices with created edges. The figure shows intuitively that the maximum length of the edges takes the value of the upper boundary $L/2$ and that the mean length of the edges also takes an approximately constant value. This behavior suggests that the net decrease ratio in edges h is approximately zero because the net removal of edges is considered to be accompanied by the fluctuation in the value of the longest length of edges. Then, the phenomenological equation for edge length distribution for this case is as follows:

$$\frac{\partial E(l,t)}{\partial t} = D\frac{\partial^2 E(l,t)}{\partial l^2}. \tag{9}$$

Here, the boundary condition for $E(l)$ is the adiabatic condition, $\frac{\partial E(l \simeq 2,t)}{\partial l} = \frac{\partial E(l=L/2,t)}{\partial l} = 0$, because the number of created edges is nearly constant after entering the second stage of network evolution. The numerically obtained time evolutions of the edge length distribution, some of which are illustrated in Fig. 7(b), are consistent with the analytical solution of (9) for both the adiabatic boundary condition and the initial condition, wherein $E(l) \sim N - l$, which is the edge length distribution in the first stage of network evolution. (The initial time for the analytical solution must be adjusted artificially to the time when the second stage begins.) There is a mismatch between the analytical solution and the numerical data, however, especially in the region of $l = 2 \sim 4$. The reason for this mismatch is that the number of edges is influenced by the singular point at which $P(l = 1) = L$ for the periodic condition and at which $P(l = 1) = \infty$ for the free boundary condition. Therefore, it is not possible to apply (4) and (9) directly to this region. This region acts as a heat bath, which provides new edges of small length to the l space for the free boundary condition, whereas, for the periodic condition, the area outside this region is not seriously affected by this region.

Returning to the free boundary cases, we must be aware that there is no reason to distinguish the free boundary condition and the periodic boundary condition until the number of vertices with created edges reaches the period interval of the 1-D lattice. The maximum length of edges is limited by the periodicity when the periodic boundary condition is imposed, and the maximum length in the second stage of network evolution is also limited by the range of location of vertices that can add created edges. Therefore, at least until the end of the second stage, the appropriate equation that describes the time evolution of edge length distribution must be (9) even for free boundary conditions. After entering the third stage of network evolution, parameter h in (4) must begin to approach its equilibrium value. Although an appropriate equation to describe the time evolution of h has not yet been found, the changes in h can be related to the differentiation of the edge length distribution through the boundary condition (6).

V. Other Properties

In this section, some properties that provide valuable information on the network topology, namely, the shortest path length, the sum of the edge lengths along shortest paths, the clustering coefficient, and the mean local clustering $C(k)$ over vertices of degree k, are determined.

A. Shortest Path Length and the Sum of Edge Lengths on the Shortest Path

The shortest path length between vertex i and vertex j, n_{ij}, is defined as the minimum number of edges on paths that connect i and j. The mean shortest path length $\langle n_{ij} \rangle$ is then defined by

$$\langle n_{ij} \rangle = \frac{1}{N(N-1)} \sum_{i \neq j} n_{ij}, \tag{10}$$

where the summation is performed over vertices with created edges, i and j, because our interest is in the subgraph consisting of vertices with created edges.

The shortest path length is reduced by adding new edges to the initial lattice for any i and j, but the sum of Euclidian edge lengths along the shortest path tends to become larger than that for the initial lattice for any i and j, because we are treating a 1-D lattice. We estimate the degree of expansion of the Euclidian distance via the shortest path as follows:

$$\left\langle d_{ij}/d^o_{ij} \right\rangle = \frac{1}{N(N-1)} \sum_{i \neq j} \frac{d_{ij}}{d^o_{ij}}, \tag{11}$$

where d_{ij} is the sum of Euclidian edge lengths along the shortest path between vertex i and vertex j in the subgraph, and d^o_{ij} is that for the initial lattice. This formula has been used to investigate the efficiency in spatial networks [17]. We also calculate the mean edge length over edges along the shortest path $\langle d_{ij}/n_{ij} \rangle$,

$$\langle d_{ij}/n_{ij} \rangle = \frac{1}{N(N-1)} \sum_{i \neq j} \frac{d_{ij}}{n_{ij}}, \tag{12}$$

which express the length of typical edges that frequently occur in shortest paths.

Figure 8 presents the results of the calculation of these values for graphs for which the changes in maximum edge length are presented in Fig. 3. Figures 8(a) and 8(b) show that both $\left\langle d_{ij}/d^o_{ij} \right\rangle$ and $\langle d_{ij}/n_{ij} \rangle$ keep pace with the changes in mean length of edges with considerable accuracy. Considering that increases in mean edge length are associated with increases in the maximum length of edges, as mentioned in Subsection IV-A, this result implies that the creation of long edges contributes to the production of short paths with a circuitous route measured by the edge length. As for the mean shortest path length, which is shown in Fig. 8(c), the change in the shortest path length does not exhibit a sensitive response to changes in mean edge length. Instead, Fig. 8(c) exhibits instantaneous increases in mean shortest path length, which implies that graphs with a large mean shortest path length are in an unstable state, the structure of which can only be maintained for a short time interval. (For example, based on Fig. 8(c), $\langle n_{ij} \rangle \simeq 3 \sim 4$ appears to be unstable.)

These results for time dependence can be interpreted based on the assumptions in the model, according to which it is difficult for the walker to reach to a certain vertex via several edges, although there is no limit on the length of edges that the walker passes. Therefore, the movement of the walker can respond to increases in $\langle n_{ij} \rangle$ by not moving toward an unapproachable area, although the movement of the walker is

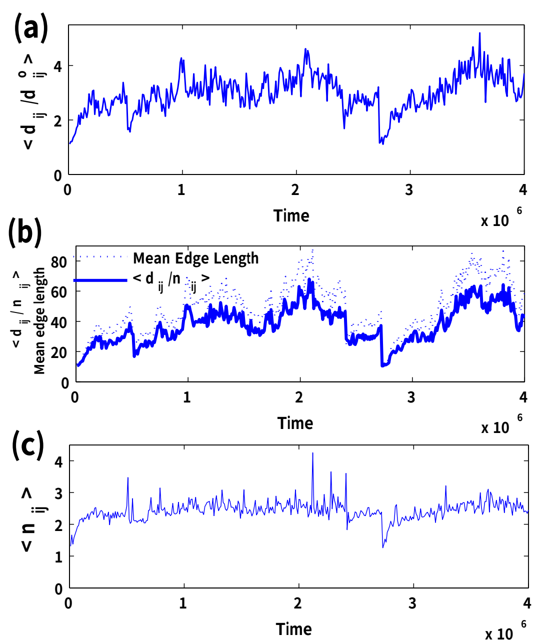

Fig. 8. Time dependence of the degree of expansion of Euclidian distance via the shortest path $\left\langle d_{ij}/d^{o}_{ij}\right\rangle$, mean edge length along shortest paths $\langle d_{ij}/n_{ij}\rangle$, and mean shortest path length $\langle n_{ij}\rangle$. The calculation is performed for the same data used in Fig. 3 ($p_{\rm d} = 0.004$). (a) $\left\langle d_{ij}/d^{o}_{ij}\right\rangle$. (b) $\langle d_{ij}/n_{ij}\rangle$ and mean edge length (reprint of Fig. 3). (c) Mean shortest path length $\langle n_{ij}\rangle$.

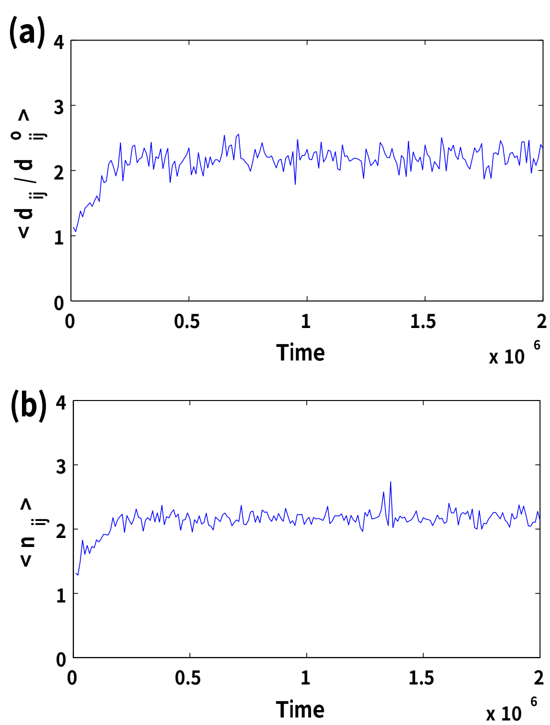

Fig. 9. Time dependence of the degree of expansion of the Euclidian distance via the shortest path $\left\langle d_{ij}/d^{o}_{ij}\right\rangle$ and the mean shortest path length $\langle n_{ij}\rangle$ under the periodic boundary condition with a period of 101 ($p_{\rm d} = 0.004$). (a) $\left\langle d_{ij}/d^{o}_{ij}\right\rangle$. (b) Mean shortest path length $\langle n_{ij}\rangle$.

not influenced by the edge length that the walker passes. As a result, instantaneous increases in $\langle n_{ij}\rangle$ can be interpreted as a sign of removal of a part of the subgraph consisting of vertices with created edges, because the unapproachable area for the walker continuously loses created edges. In comparison, the results for $\left\langle d_{ij}/d^{o}_{ij}\right\rangle$ and $\langle d_{ij}/n_{ij}\rangle$ suggest that increases in these values only increases the risk of accidental creation of unapproachable areas, although these increases do not directly affect the movement of the walker.

For cases of the periodic boundary condition, not only $\langle n_{ij}\rangle$, but also $\left\langle d_{ij}/d^{o}_{ij}\right\rangle$, exhibits stable changes in time, as indicated in Figs. 9(a) and 9(b). In this case, in contrast to the cases of free boundary conditions, control of the maximum length of edges induced by the periodicity of the lattice results in a stabilization of changes in the mean shortest path length. The stabilization of changes in these values provides a basis for the condition $h = 0$, which was assumed in the derivation of (9), because stabilization of changes in mean shortest path length is equivalent to controlling the occurrence of areas that are unapproachable by the walker.

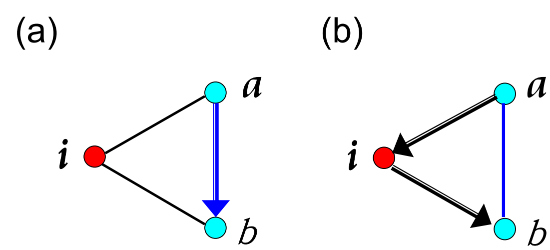

Fig. 10. Processes adding strength to edges connecting two adjacent vertices of vertex i. (a) Walkers passing through an edge that connects two adjacent vertices, a and b, of vertex i. This process strengthens the edge between a and b by 1 (b) Walkers passing vertex i. This process strengthens not only edges passed by the walker but also edges between a and b by 1.

B. Clustering Coefficient

The local clustering strength c_i of a vertex i of degree k_i is defined as follows:

$$c_i = \frac{2e_i}{k_i(k_i-1)}, \qquad (13)$$

where e_i denotes the number of edges that directly connect two adjacent vertices of vertex i. The mean clustering strength C is defined as the average of c_i taken over all vertices under consideration, and $C(k)$ is defined as the average of c_i taken over all vertices of a given degree k. The clustering strength measures the local group cohesiveness and yields valuable information on the networks structure because $C(k)$ exhibits non trivial behavior in real networks. For example, the power law behavior in $C(k)$ is reported for several cases, including biological networks [18] ($C(k) \sim k^{-2}$), the language network [19] ($C(k) \sim k^{-1}$), the Internet at the AS level [20] ($C(k) \sim k^{-0.75}$), and technological networks [19] ($C(k)$ is nearly constant).

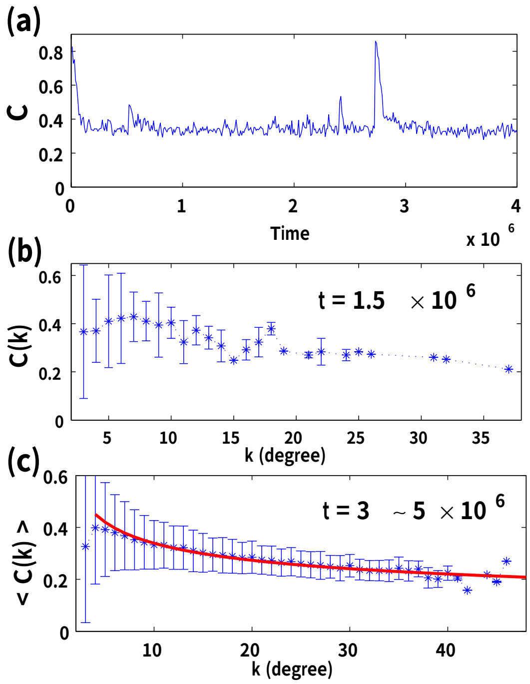

Fig. 11. Mean clustering strength C and $C(k)$. The calculation is performed using the same data as in Fig. 3 ($p_{\mathrm{d}} = 0.004$). (a) Time dependence of mean clustering strength when $p_{\mathrm{d}} = 0.004$. The instantaneous increase observed at $t \simeq 2.8 \times 10^6$ corresponds to a temporal reduction in the subgraph by the removal of edges and vertices with long created edges on a broader scale than that shown in Fig. 4. (b) $C(k)$ and the standard deviation of c_i with vertex degree k ($t = 1.5 \times 10^6$). (c) $C(k)$ averaged over 200 graphs in $t = 3 \sim 5 \times 10^6$ and the standard deviation of c_i with vertex degree k. The fitting curve superimposed in this figure is estimated as $\sim k^{-0.31}$.

In the model under consideration, $C(k)$ can be related to the frequency of the passage of the walker near a vertex of degree k by considering the balance between the decrease in the sum of the strengths over edges that directly connect two adjacent vertices of vertex i and the increase in this sum ΔA_i,

$$\Delta A_i = \frac{k_i(k_i - 1)C(k_i)p_{\mathrm{d}}}{2}. \qquad (14)$$

Here, ΔA_i can be interpreted as being proportional to the frequency of the passage of the walker over or near vertex i, because the passage of such a walker strengthens edges that directly connect two adjacent vertices of vertex i (See Fig. 10). Of course, the identity (14) does not always hold for all vertices i. The identity is only valid for cases in which the rate of change of the right-hand side is far smaller than the time scale $1/p_{\mathrm{d}}$.

Figure 11(a) illustrates the time dependence of the mean clustering strength over all vertices with created edges. As shown in the figure, after the collapse of the nearly complete subgraph, the mean clustering strength immediately reaches its equilibrium value, which is in the range 0.3 to 0.4.

Figures 11(b) and 11(c) shows the dependency of $C(k)$ on the value of vertex degree k. Roughly speaking, the figure shows that $C(k)$ can take large values regardless of the value of vertex degree k, although the $k-$dependence is estimated to be $\sim k^{-0.31}$ in the calculation. As k increases, the standard deviation of $C(k)$ decreases. This constancy of $C(k)$ with respect to k implies that the time dependence of the local clustering strength of a vertex of large degree is also nearly constant with respect to time, because the vertices of the largest k must have evolved slowly via vertices of smaller vertex degrees. Therefore, the results support the validity of identity (14), especially when k is large. The constancy of $C(k)$ with respect to k and (14) reveal that the frequency of the passage of the walker near vertex i, ΔA_i, depends roughly on k in the form $\sim k^2$. Such an ability of vertices of large degree to attract a walker is thought to be necessary for the long lifetime of such vertices of large vertex degree, are associated with the occurrence of long edges. The creation of shortcuts caused by the movement of the walker provides not only a control of the global topology of the subgraph, but also stabilization of the local structure such as $C(k)$.

VI. Summary and Discussion

We have investigated the distribution of Euclidian edge length in networks generated by shortcuts created in a 1-D lattice after traces of a random walker on the network. We found that the edge length distribution $E(l, t)$ evolves according to the three stages of the time evolution of the graph, where l is the length of edges and t is a time variable.

In the first stage, in which a nearly complete subgraph embedded in the 1-D lattice is created by the movement of the walker, the edge length distribution takes a triangular form $E(l) \sim N - l$, where the number of vertices with created edges N evolves as $N = (6t)^{1/3}$. In the second stage, where the nearly complete subgraph collapses while maintaining the number of created edges, the edge length distribution begins to be subject to the heat conduction equation (9) with the adiabatic condition at $l \simeq 2$. (The theory is not applicable to the interval near the singular point $l = 1$, where $E(l = 1) = \infty$. Therefore, the boundary condition is imposed on $l \simeq 2$, but not just on $l = 2$.) After entering the third stage, in which not only the number of created edges, but also the number of vertices with created edges, are in an equilibrium state, a radiation term $-hE(l, t)$ appears in the heat conduction equation indicated in (4). As a result, for a stationary condition $\frac{\partial}{\partial t}E(l, t) = 0$, the solution $E(l, t = \infty)$ is an exponential function that shows that the equilibrium distribution is stabilized by the balance between the diffusion rate of the edge length and the lifetime of edge length in the l space. Compared to the numerically obtained data, we concluded that $D\tau \sim 1/p_{\mathrm{d}}^2$, where τ is the lifetime of the edges in l space, and D is the rate of diffusion of the edges in l space, which shows that τ increases rapidly as $p_{\mathrm{d}} \to 0$. If the maximum length of edges is limited by the periodicity of the initial lattice with a period smaller than the characteristic length of edges determined by the above case, the equilibrium distribution of the edge length is a uniform distribution that is a stationary solution of (4).

Considering that the time scale of changes in the edge length distribution is far larger than that for the movement of the walker, the diffusion image of edges in l space will never be realized without the frequent visitation of the walker to each vertex with created edges. In other words, the diffusion image is a consequence of the statistics of the walker visiting vertices.

The calculation of the mean shortest path length suggests that the subgraph is maintained in a state such that the walker can easily visit all vertices in the subgraph. Such a large traffic capacity enables the subgraph to exist in a widespread structure in the 1-D lattice as well as the long lifetime of vertices of large degree. Even if an unapproachable area for the walker accidentally appears in the subgraph, the unapproachable area will immediately become extinct. Such a natural extinction of the unapproachable area for the walker is associated with the removal of a number of edges and circuitous routes with long edges. The movement of the walker provides the subgraph with an automatic control with which to maintain the large traffic capacity in the subgraph. The calculation of the clustering strength also shows that $C(k)$ takes large values regardless of the value of vertex degree k. This result not only indicates that that movement of the walker stabilizes the local structure of the subgraph, but is also considered to be an indicator of such a large traffic capacity for every vertex in the subgraph.

Note that 1-D lattices are a very special case. According to previous research [15], similar models on two-dimensional and three-dimensional lattices exhibit different behaviors regarding the traffic capacity of the subgraph, even when $p_{\mathrm{d}} = 0$. Therefore, the results obtained in the present study should be considered to be unique to 1-D cases.

Note also that the random transports modeled by a random walker are extreme in that the vertices are only waiting for visits by the transports. Transports (or transmission of information) in networks can be modeled in various manners. With respect to the random walker model, a walker might be aware of the length of edges that the walker passes. The development of stochastic models of networks considering such transports should therefore be an interesting subject to study.

REFERENCES

[1] M. E. J. Newman, The structure and function of complex networks, *SIAM review* 45, 2003, pp. 167–256.

[2] Gheorghe Grigoras, Gheorghe Cartina, Marcel Istrate, Florina Rotaru, The Efficiency of the Clustering Techniques in the Energy Losses Evaluation from Distribution Networks, *International Journal of Mathematical Models and Methods in Applied Sciences* 5, 2011, pp. 133–141.

[3] L. Vasek, V. Dolinay, Simulation Model of Heat Distribution and Consumption in Municipal Heating Network, *International Journal of Mathematical Models and Methods in Applied Sciences* 4, 2010, pp. 240–248.

[4] S. Boccalettia, V. Latorab, Y. Morenod, M. Chavezf, D.-U. Hwanga, Complex networks: Structure and dynamics, *Physics Reports* 424, 2006, pp. 175–308.

[5] A.-L. Barabási and R. Albert, Emergence of scaling in random networks, *Science* 286, 1999, pp. 509–512.

[6] D. J. Watts and S. H. Strogatz, Collective dynamics of ‘small-world’ networks, *Nature* 393, 1998, pp. 440–442.

[7] R. Guimera, S. Mossa, A. Turtschi, and L. A. N. Amaral, The world-wide air transportation network: Anomalous centrality, community structure, and cities’ global roles, *Proc. Natl. Acad. Sci. USA* 102, 2005, pp. 7794–7799.

[8] M. T. Gastner and M. E. J. Newman, The spatial structure of networks, *Euro. Phys. J. B* 49, 2006, pp. 247–252.

[9] J. Quartieri, M. Guida, C. Guarnaccia, S. D’Ambrosio and D. Guadagnuolo, Topological Properties of the Italian Airport Network studied via Multiple Addendials and Graph Theory, *International Journal of Mathematical Models and Methods in Applied Sciences* 2, 2008, pp. 312–316.

[10] S. Jespersen and A. Blumen, Small-world networks: Links with long-tailed distributions, *Phys. Rev. E* 62, 2000, pp. 6270–6274.

[11] P. Sen, K. Banerjee, and T. Biswas, Phase transitions in a network with range dependent connection probability, *Phys. Rev. E* 66, 2002, pp. 037102.

[12] N. Ikeda, Network formed by traces of random walks, *Physica A* 379, 2007, pp. 701–713.

[13] N. Ikeda, Network formation determined by the diffusion process of random walkers, *J. Phys. A : Math. Theor.* 41, 2008, pp. 235005(18pp).

[14] N. Ikeda, Control of network structure by an external field on random walkers, *Proceedings of the 6th WSEAS International Conference on Non-Linear Analysis, Non-Linear Systems and Chaos, Arcachon, France, 2007*, pp. 85–90.

[15] N. Ikeda, Impact of initial lattice structures on networks generated by traces of random walks, *Physica A* 389, 2010, pp. 3336–3347.

[16] A. Sommerfeld, *Partial Differential Equations in Physics*, Academic press, 1949, ChapterIII.

[17] M. T. Gastner and M. E. J. Newman, Shape and efficiency in spatial distribution networks, *J. Stat. Mech.* , 2006, pp. 01015.

[18] S.H. Yook, Z.N. Oltvai, and A.-L. Barabási, Functional and topological characterization of protein interaction networks, *Proteomics* 4, 2004, pp. 928–942.

[19] E. Ravasz and A.-L. Barabási, Hiearchical organization in complex networks, *Phys. Rev. E* 67, 2003, pp. 026112.

[20] A. Vázquez, R. Pastor-Satorras, and A. Vespignani, Large-scale topological and dynamical properties of the internet, *Phys. Rev. E* 65, 2002, pp. 066130.